DOI 10.31489/2022No2/48-57

UDC 536.7, 536.245

DEVELOPMENT AND RESEARCH OF THE TOPOLOGY OF COOLING BAFFLES FOR BLADES OF THE AXIAL CARBON DIOXIDE TURBINES

Komarov I.I., Vegera A.N., Bryzgunov P.A.*, Makhmutov B.A., Smirnov A.O.

National Research University "Moscow Power Engineering Institute", Moscow, Russian Federation, BryzgunovPA@mpei.ru

Currently, there is an increase in average annual temperature and climate change across the various continents. Carbon dioxide emissions from energy facilities contributed to this condition. Implementation of oxy-fuel cycles is a promising solution for reducing carbon dioxide emissions from the energy sector. To date, the most efficient oxy-fuel cycle is the Allam cycle. In this cycle supercritical carbon dioxide acts as a working fluid of the cycle, wherein CO_2's temperature upstream of the turbine is 1,150 °C and the pressure is 30 MPa. Due to the high temperature of the working fluid, it is necessary to cool first stages of the carbon dioxide turbine. The feature of considered cooling system in this turbine is that carbon dioxide being used as a refrigerant too. This paper investigated two topologies of convective cooling systems in the carbon dioxide turbine's nozzle blade as well as considers an option for increasing the intensity of heat exchange through the use of helical ribbing in the cylindrical cooling baffle. Numerical simulation involving the ANSYS software package was performed for two topologies of the cooling baffles arrangement in the nozzle blade body: configuration 1 - with 17 baffles of 1 mm diameter, configuration 2 - with three baffles of the blade profile shape. Configuration 1 proved to be more efficient: the Nusselt number has a value of 117, and average value of the heat transfer coefficient on the refrigerant side is 6,413 $W/m^2 \cdot K$. The effect of using helical ribbing in the cooling cylindrical baffle of the blade under study was investigated, which enabled to reduce the metal temperature by 54 °C on average and doubled the heat transfer coefficient.

***Keywords**:* cooling blade, supercritical carbon dioxide, oxy-fuel combustion power cycle, carbon dioxide turbine, rib turbulators, heat transfer.

Introduction

One of the main causes of global warming and climate change in the world is the burning of fossil fuel such as oil, coal, gas, to generate electricity [1]. Combustion of various fuels generates the greenhouse gas - carbon dioxide (CO_2). Due to economic growth, the need for electricity increases every year, [2] leading to higher consumption of natural resources. To curb the rise in average annual temperature and reduce greenhouse gas emissions, an international agreement has been adopted to limit temperature increase by 2°C by 2040 [3]. Presently, main processes to reduce the carbon dioxide emissions include: commissioning of renewable energy sources and cut down the number of power plants operating on fossil fuels; commissioning of nuclear power plants, implementation of CO_2 capture procedures. Each of the above processes has its own disadvantages. For instance, the amount of electricity generated by wind and solar power plants is highly dependent on external weather conditions [4]. These plants also face problems with integration into power network [5]. Besides, there are complications with disposal of solar batteries and blades of wind generators. Nuclear power plants have no harmful effects on climate change, but after operation the fuel must be disposed of since there is still no technology for complete recycling of the fuel [6]. Decarbonization technology (CCS) imposes high capital and operating costs on energy facilities [7]. Application of the oxygen-fuel cycles is an alternative option for reducing CO_2 emissions [8, 9]. Allam cycle is the most promising and efficient.

Based on the Brayton cycle, the Allam cycle's working fluid is the supercritical carbon dioxide. The Allam cycle power plant consists of compressor, pump, combustion chamber, carbon dioxide turbine and regenerative heat exchanger. A distinctive feature of this cycle's combustion chamber is the presence of three inlet streams: natural gas (fuel), oxygen (oxidizer) and carbon dioxide (maximum temperature limiter). Another feature of the combustion chamber is zero nitrogen content to prevent generation of NO_x. Air separating unit is used for the generation of oxygen. Downstream of the combustion chamber the combustion products consisting mainly of CO_2 at a temperature of 1,150 ° C and a pressure of 30 MPa, enter the turbine rotating the electric generator [10]. Downstream of the turbine, the exhausted carbon dioxide enters the regenerative heat exchanger, and then into the water separator, where the condensed steam is removed. Then, one portion of the gas is returned to the cycle, and another portion is sent for disposal [11,12]. Thus, no CO_2 greenhouse gas emissions take place.

Allam cycle's carbon dioxide turbine is notable for parameters of working fluid upstream of the first stage. Pressure of the combustion products corresponds to parameters of steam turbines at supercritical parameters, and the working fluid temperature is similar to gases at the gas turbine inlet. Due to these parameters it is necessary to apply additional cooling of the turbine rotor, nozzle and rotating blades of first stages [13]. The turbine cooling is notable for using CO_2 as a refrigerant. Unlike air, carbon dioxide has a higher density (by 35%) and this must be taken into account when designing the turbine cooling system, because due to the higher density it may be difficult to form a film on the blade wall. Toshiba Company, being designer of combustion chamber and carbon dioxide turbine of the Allam cycle for blade cooling, suggests the loop convective cooling circuit without film cooling and with further refrigerant ejection through the blade periphery [14].

Presently, there are few publicly available studies on carbon dioxide flow in the blade cooling baffles. Main CO_2 studies cover the application of various heat exchange intensifiers [15] or analysis of gas dynamic properties of the working fluid in inter-blade baffles of the carbon dioxide turbine [16]. There are many papers on the study of various topologies of convective blade cooling systems, but air [17,18]or steam is considered as a refrigerant [19,20].

There is a large quantity of works related to studying of heat exchange intensifiers. The paper [21] contains large study of different rib shapes with various installation angles in the baffle. V-rib with 60° installation angle shows the highest thermal-hydraulic performance. The article [22] compares thermal hydraulic properties of round, oval, ellipsoid and drop-shaped pins. The drop-shaped pin is the most efficient under the same conditions. Paper [23] gives a brief overview of commonly used heat transfer intensifiers, suggesting the use of slots and curved ribs as an alternative to inclined ribs and pins. In the considered articles on heat exchange intensifiers the studies are conducted in rectangular baffles. Not much work has been done in circular baffles, although the shape of the cooling baffle may greatly influence the flow of refrigerant in it. The paper [24] studies ribs installed at right angles in baffle with the circular cross section. Thanks to the ribbing under review, it was possible to increase the heat transfer coefficient by the flow transition and increasing the area of heated surface. Similar paper is given in the article [25], only the configuration with ribs located along the baffle was investigated. Use of ribs in the cooling baffle has increased the cooling efficiency of the turbine blade. The article [26] studied two baffles: one with oblique ribs and the other with V-shaped ribs. The average Nusselt number is much higher in the configuration with V-shaped ribs due to the formation of many vortices, while in the configuration with oblique ribs only one vortex is formed.

This paper deals with the study of two different topologies for convective cooling of carbon dioxide turbine blades. Cooling system designs will differ in the location and size of baffles in the blade body. Also, to increase the intensity of convective heat transfer, a new design of intensifier was developed and tested: helical ribbing. The study was conducted for a baffle similar to the baffle of the cooled configuration 1 blade. Carbon dioxide will be used as a refrigerant with parameters corresponding to parameters of the Allam CO_2 cycle.

1 Geometry

Two topologies for the arrangement of cooling baffles in the nozzle blade were designed for the study: a configuration with 17 baffles having diameter of 1 mm spaced 5 mm apart (configuration 1) and a configuration with three baffles the shape of which is the same as shape of the blade profile (configuration 2). Profile of the C-9015A nozzle set has been selected for accommodation of baffles in the blade body. The wall thickness between cooling baffles and the outer wall of the blade airfoil is 1 mm in both cases. Basic geometry, such as chord and blade height, are also equal and shown in Table 1. The cross-sectional area of the cooling space in the configuration with three baffles is 200 mm^2, while in the baffle of 1 mm diameter it is 13.4 mm^2. Schematic designs of both configurations are shown in Figures 1 and 2.

Due to economic growth, the need for electricity increases every year, [2] leading to higher consumption of natural resources. To curb the rise in average annual temperature and reduce greenhouse gas emissions, an international agreement has been adopted to limit temperature increase by 2°C by 2040 [3].

.

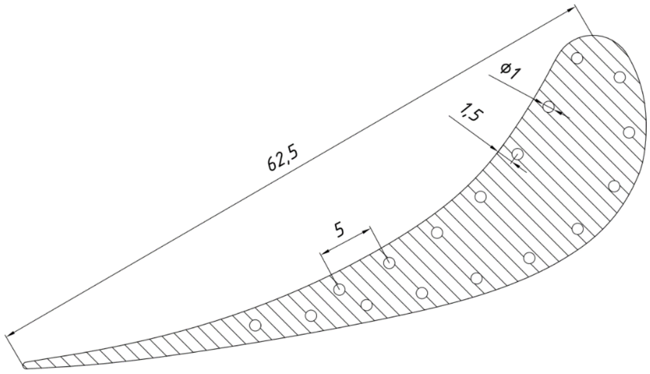

Fig.1. Cross-section of the blade under study with baffles of 1 mm diameter.

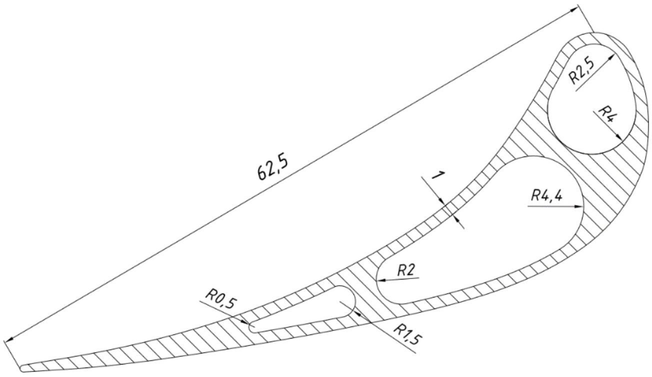

Fig.2. Cross-section of the blade with three baffles under study.

Table 1. Basic geometry of blades under study.

Type of design	Diameter of baffles, mm	Baffles pitch, mm	Number of baffles	Wall thickness, mm	Profile chord, mm	Blade height, mm
Configuration 1	1	5	17	1	62.5	25
Configuration 2	-	-	3			

To increase the efficiency of cooling in the configuration 1 blade, the effect of heat transfer intensification inside the cylindrical baffle was studied. Use of the heat exchange intensifiers results in flow mixing and transition, thus improving heat transfer from the hot walls of the blade metal to the refrigerant.

To define the increase in cooling efficiency when using intensification in the cylindrical baffle, two baffle topologies were calculated: smooth baffle and similar baffle with helical ribbing. Dimensions of the studied baffles correspond to baffles of the configuration 1 blade. Schematic designs of the studied channel models are shown in Figure 3, and Table 2 shows their basic geometrical characteristics.

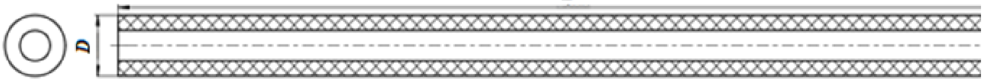

a) sketch of the circular smooth baffle

b) sketch of the circular baffle with helical ribbing

Fig.3. Geometry of studied baffles.

Table 2. Geometry parameters of studied baffles.

Parameter	Value
Baffle length, mm	25
Baffle diameter, mm	1
Wall thickness, mm	1
Helical ribbing height, mm	0.3
Helical ribbing thickness, mm	0.1
Pitch, mm	1

2 Mesh

The modelling was performed in the coupled formulation. To implement this method, a separate grid was constructed for each volume element of the model: for the blade body, for the main flow of supercritical CO_2, for the cooling baffles with supercritical CO_2. The nozzle blade body grid is entirely made of tetrahedron-shaped elements. The grid of gas flows is combined: elements of the main flow have a tetrahedron shape and the near-wall elements are prismatic in shape for more accurate calculation in the boundary layer zone. Indicator of grid quality in the boundary zone is the y^+ value, which should be close to 1. For similar conditions at the stage inlet the CO_2 density is twice higher than air density, at the average. As a result, height of the first boundary layer in grid near the blade wall of turbine operating on supercritical carbon dioxide is twice less than for conventional gas turbines with the same y^+ [16]. To achieve a low y^+ value, a grid model with a large number of elements is required. To speed up the calculation and reduce the number of grid elements at the upper and lower flow boundaries, no additional prismatic boundary layers which significantly increase the volume of the grid model, were created. Main characteristics of the calculation model grid with 1 mm diameter baffles and of the computational model with three baffles in the form of blade profile are presented in Table 3. Figure 4 shows the computational grid of the configuration 1 blade.

The Ansys software package was used to study the effect of heat exchange intensification in the cylindrical baffle. The computational grid is volumetric, unstructured, tetrahedral. Method for designing the computational grid of models under study is Delaunay. Prismatic boundary layer is modeled on the baffle walls and on helical ribbing. Figure 5 shows the computational grid of the baffle with helical ribbing.

Table 3. Main characteristics of the studied topologies computational grids.

Parameter	Value	
	Configuration 1	Configuration 2
Number of grid elements, mln.	8,028	7,698
Blade body		
Global size of the grid, mm	0.33	0.23
Working fluid flow		
Global size of the grid, mm	0.58	0.55
Prismatic layer design procedure	First Layer Thickness	
First prismatic layer thickness, mm	0,017	0,007
Number of prismatic layers	13	14
Growth rate	1.26	1.3
Boundary layer design algorithm	Pre	
Cooling baffles		
Global size of the grid, mm	0.1	0.18
Prismatic layer design procedure	First Layer Thickness	
First prismatic layer thickness, mm	0,006	0,0045
Number of prismatic layers	10	12
Growth rate	1.2	1.28
Boundary layer design algorithm	Pre	

.

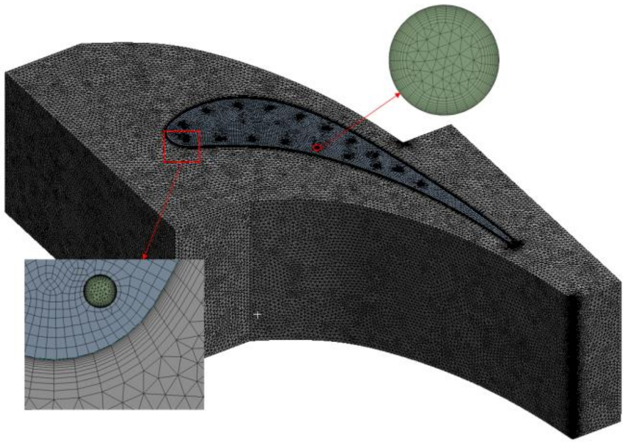

Fig.4. Reference Grid of the Configuration 1 blade.

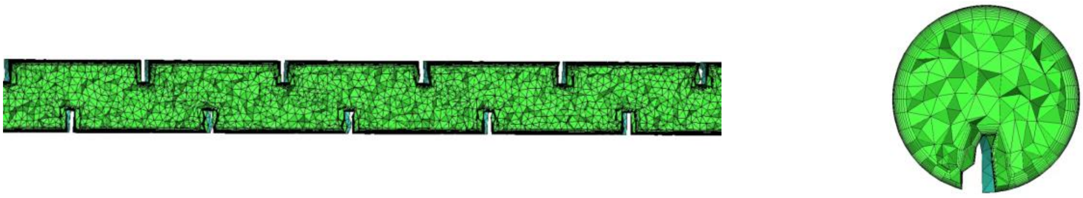

a) Longitudinal Section b) Lateral Section

Fig.5. Reference Grid of the Baffle with Helical Ribbing.

3 Boundary and Physical Conditions

The boundary conditions in use herein are compliant with the fluid parameters of the Allam cycle carbon dioxide turbine [8]. The full braking pressure and temperature are set for the primary carbon dioxide flow in the inter-blade baffle while the static pressure is set for the output. The full braking pressure and temperature are also set for the input cooling baffles while the total coolant consumption is set for the baffle outputs. In addition to physical parameters of the fluid, the density of the blade material equal to 8050 kg/m^3, the specific heat equal to 573 J/kg·K, and the heating constant equal to 22.1 W/m·K were set. These material specifications correspond to the nickel-based Alloy 740. For the primary specifications of the boundary conditions, see Table 4. The periodic boundaries were set for the side surfaces of the primary carbon dioxide flow. Figure 6 shows the reference model for research of the blade with cooling baffles 1 mm in diameter under the set boundary conditions. The calculation uses the turbulence model *k-ω* SST.

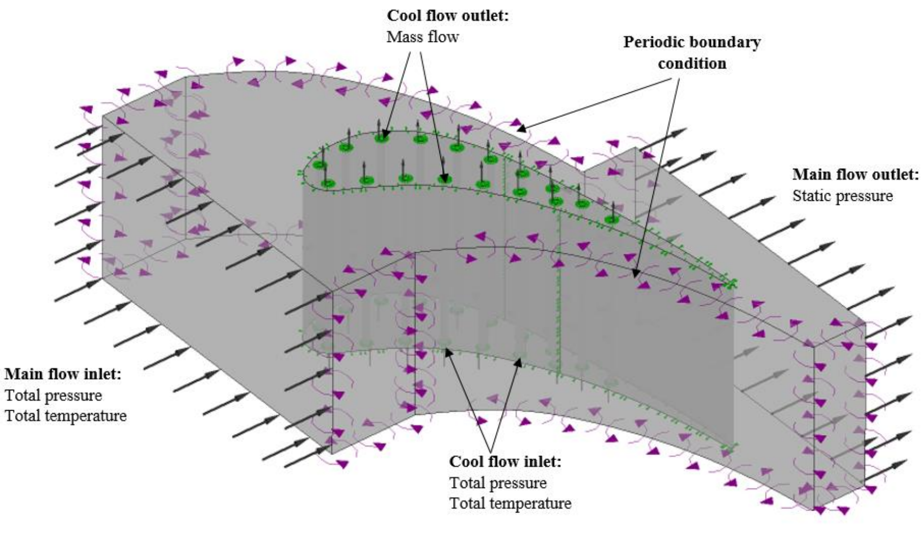

Fig.6. Boundary Conditions of the Reference Model

Table 4. Reference Boundary Conditions.

Parameter	Value
Primary Flow Input Pressure, MPa	30
Primary Flow Input Temperature, K	1373.15
Primary Flow Output Pressure, MPa	25
Cooling Baffle Input Pressure, MPa	30
Cooling Baffle Input Temperature, K	473.15
Total Coolant Consumption at Cooling Baffle Outputs, kg/sec	0.0224
Primary Flow and Coolant Material	S-CO2
Blade Body Material	Alloy 740
Turbulence Model	SST

The boundary conditions for the mathematical model of the cylindrical baffles on review were selected in accordance with the carbon dioxide parameters of the Allam cycle carbon dioxide turbine. Carbon dioxide flow modelling used the Ansys CFX mathematical package. For the boundary conditions of the reference model, see Table 5. The k-ω SST was used as the turbulence model. Mean outer wall temperatures were set for modelling heat and hydrodynamic processes of the baffles on review. The full braking pressure and the flow temperature were set for the baffle input while the coolant consumption depending on the Reynolds number was set for the output section. The calculations were conducted within the *Re* number range from 20000 to 100000 in increments of 20000.

Table 5. Boundary Conditions for Cylindrical Baffle Calculations.

Parameter	Value
Fluid	CO_2
Baffle Input CO2 Temperature, °C	200
Baffle Input Pressure, MPa	30
Wall Temperature, °C	850
Reynolds Number	20000, 40000, 60000, 80000, 100000
Turbulence Model	SST

4 Methods

The thermal transmittance value was calculated to analyze the influence of helical ribbing usage in the cylindrical cooling baffle on the blade metal temperature. The inputs for the analysis were the Ansys CFX computational flow dynamics results for the cooled configuration 1 blade. To calculate the coolant thermal transmittance value, the baffle was selected which is located in the immediate proximity of the most heat-loaded zone while the wall element between two baffles throughout the blade height was selected in the same zone to calculate the fluid thermal transmittance value.

First, the thermal transmittance values were determined for the coolant and for the hot gasses. After the thermal transmittance values were determined, the heating constant was determined for the design with smooth baffles and for the baffle with helical ribbing subject to variations of the thermal transmittance value directly proportional to the Nusselt number. Finally, we were able to compute the wall temperature resulting from usage of helical ribbing in cylindrical cooling baffles of the nozzle blade.

5 Results and Discussion

This study provides mathematical modelling of two convective cooling configurations for the nozzle blade of the carbon dioxide turbine. The least blade metal temperatures are achieved under the topology with 17 cooling baffles 1 mm in diameter. The mean volumetric temperature of the metal is achieved under configuration 1 and equals 1218 K while in configuration 2, the mean temperature equals 1331 K or 9.5 % higher than that of configuration 1. The minimum metal temperature in the 17-baffle configuration equals 978 K or 12.2 % lower than that of the three-baffle configuration (Figure 7).

The 17-baffle convective cooling system also demonstrates higher heat exchange intensity versus the three-baffle configuration. In configuration 1, the *Nu* value equals 117 while in configuration 2, it equals 68 (42 % lower). The thermal transmittance value is also higher for the topology with cooling baffles 1 mm in

.

diameter and it is as high as 6400 W/m^2·K. In the topology with three cooling baffles, the thermal transmittance value equals 520 W/m^2·K or 12.3 times lower versus configuration 1 (Figure 8).

The obtained results are associated primarily with the Reynolds number value of the nozzle blade cooling baffles. The Nusselt number and the thermal transmittance values are directly proportional to the *Re* value of the baffle. The higher the coolant velocity in the cooling baffles is, the higher the Reynolds number value is. It results into increasing heat exchange intensity and thermal transmittance value.

Ceteris paribus, the topologies of blade convective cooling systems on review have materially different values of significant baffle dimensions. The clear area of baffles 1 mm in diameter is significantly lower than the clear area of baffles of the configuration 2 blade. Therefore, subject to the continuity equation and under the same coolant consumption values, the velocity in the configuration 1 baffles is much higher than in the three-baffle configuration baffles. For the 17-baffle blade, the coolant velocity equals 4.2 m/sec while it is 15 times lower for the three-baffle blade and equals 0.28 m/sec. The Reynolds number of the carbon dioxide flow in the configuration 1 cooling baffles equals 23200 while it equals 12850 for the configuration 2 baffles or 45 % lower versus the first topology. For the three-baffle blade to achieve the same Reynolds number value in its cooling baffles as the configuration with 17 baffles 1 mm in diameter, the coolant consumption must be 1.8 times higher.

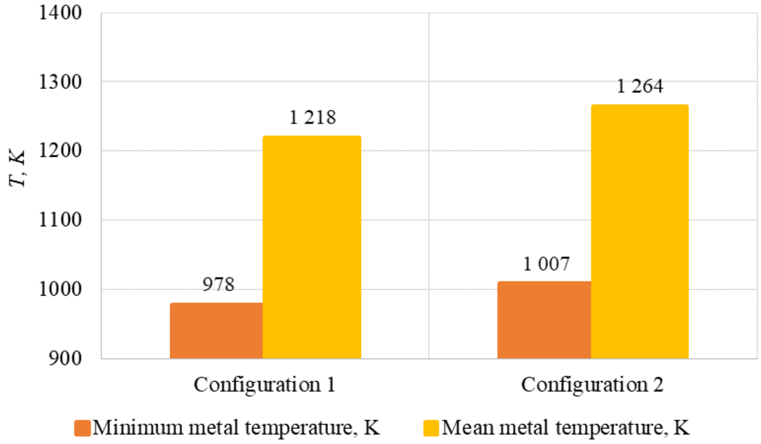

Fig.7. Dependency of the Blade Metal Temperature on the Topology of the Cooling Baffles.

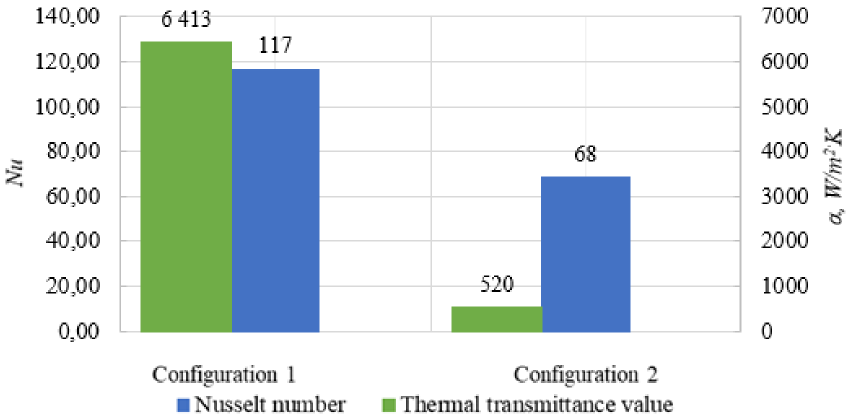

Fig.8. Dependency of the Nusselt Number and the Thermal Transmittance Values on the Topology of the Blade Cooling Baffles.

Figure 9 shows metal temperature profiles for significant sections along the blade height such as the root, middle and peripheral sections. Referring to the figure, it will be seen that it is possible to limit the influence of high primary carbon dioxide flow temperature on the airfoil interior where the lowest temperatures for the entire blade volume are achieved for the configuration 1 blade by positioning the cooling baffles along the blade profile 1 mm away from the profile wall. This topology allows to reduce the wall temperature by 100 K on the average for the concavity but not for the back and the leading edge of the blade where the wall temperature is as high as 1350 K. It is associated with the primary flow velocity along the blade back exceeding the one along the concavity, which increases the thermal transmittance value on part of hot gasses. It may also be associated with an insignificantly greater distance between the cooling baffles and the profile wall on the profile back side in the half-interval zones between the baffles. Decreasing heat exchange intensity and cooling performance are observed throughout the blade height due to the coolant heating. To increase the profile convexity cooling performance for the nozzle blade on review with this cooling baffle positioning configuration, one must reduce the intervals between the cooling baffles along the back.

Configuration 2 shows high heating of all outer walls of the blade profile. It is possible to reduce the temperature materially between the root section cooling baffles themselves only. Throughout the blade height and due to low velocity in the cooling baffles, the coolant heats rapidly and the walls between the baffles are cooled insignificantly in the middle section already. This cooling system configuration must have higher coolant consumption to achieve normal flow velocities in the baffles, and the cooling baffle walls may have heat exchange intensifiers.

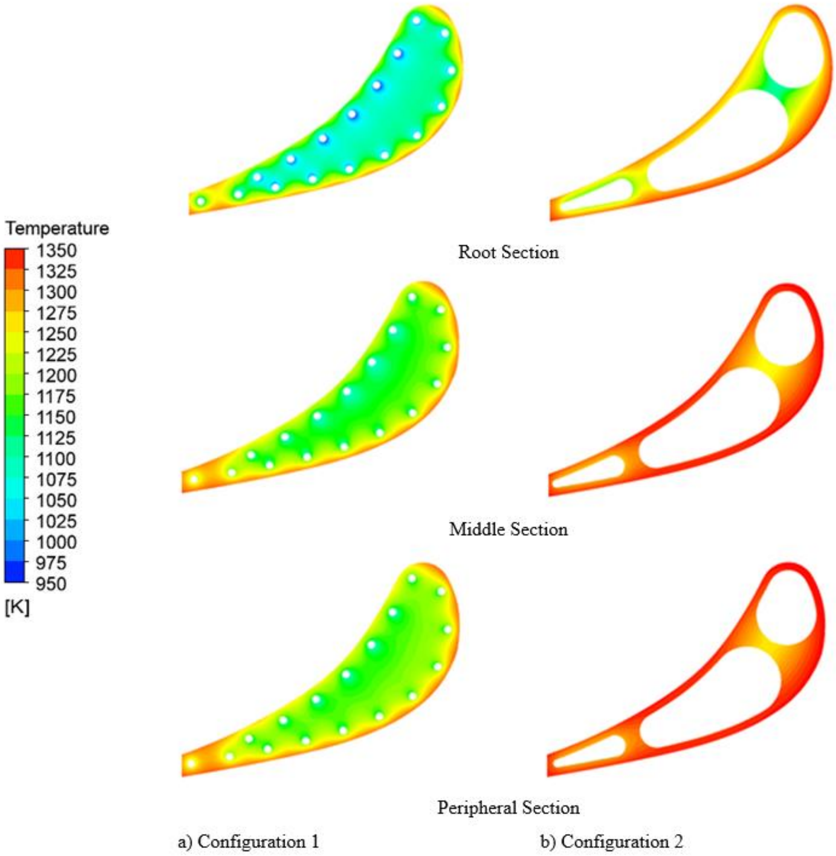

Fig.9. Temperature Profiles.

Circular baffle study results are shown as diagrams of dependency of the Nusselt number (Figure 10) and linear hydraulic loss ratio (Figure 11) on the Reynolds number. Using helical ribbing allows to increase the heat exchange intensity by 91% on the average throughout the Reynolds number range on review. The Nusselt number increases due to the coolant flow turbulence and the increasing heat exchange contact area. However, using helical ribbing increases the losses associated with the hydraulic loss ratio. In this connection, as the Reynolds number increases the hydraulic loss ratio of the cylindrical baffle with ribbing decreases by 10% due to decreasing thickness of the boundary layer. The *Re* number equals 23240 for the cooling baffle in the calculations for the configuration 1 blade. At this Reynolds number, the Nusselt number is 2 times higher for the baffle with helical ribbing, which causes the baffle thermal transmittance value to increase 2 times as well.

.

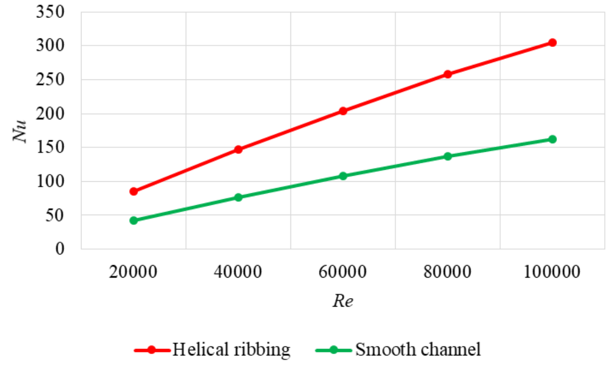

Fig.10. Diagram of Dependency of the Nusselt Number on the Reynolds Number for the Baffles on Review.

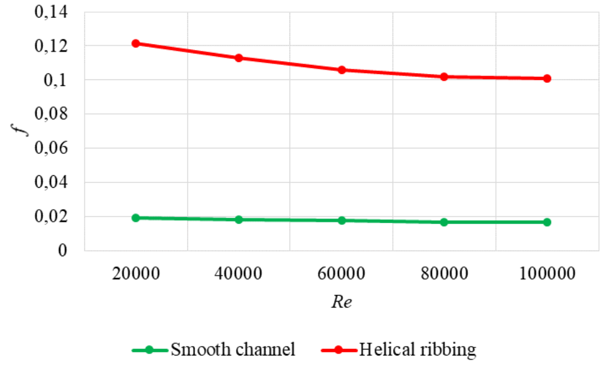

Fig.11. Diagram of Dependency of the Hydraulic Loss Ratio on the Reynolds Number for the Baffles on Review.

Using heat exchange intensification in the form of helical ribbing of the cooling baffles of the nozzle blade on review caused the wall temperature in the most heat loaded area to decrease by 54 °C. It also allowed to increase the thermal transmittance value by 33%. Due to the increasing thermal transmittance value, the helical ribbing may be used to reduce the coolant consumption for cooling at the constant blade metal temperature, which, in its turn, would cause the cycle performance to increase.

Conclusions

The following conclusions may be drawn from the completed studies:

1) The design with 17 baffles 1 mm in diameter ensures more efficient cooling of the blade than the three-baffle structure. The first topology ensures lower metal temperatures throughout the blade volume. Design 1 also has higher values of the Nusselt number (42 % higher versus configuration 2) and thermal transmittance (12 times higher). It is associated with a higher differential velocity of the coolant in the baffles of the topologies on review and thus with different Reynolds number values for them.

2) For the configuration 2 blade to achieve the similar Reynolds number value for its cooling baffles as the blade with 17 baffles, the coolant consumption must be 1.8 times higher. Therefore, the configuration ensures coolant savings, which allows to decrease the carbon dioxide turbine losses materially.

3) The 17-baffle topology clearly demonstrates non-homogeneity of cooling along the blade profile. This topology ensures much better reduction of the wall concavity temperature versus the back and the leading edge of the blade. It is associated with a higher primary flow velocity along the back of the profile versus the concavity, which increases the thermal transmittance value on part of hot gasses. It may also be associated with an insignificantly greater distance between the cooling baffles and the profile wall on the profile back side in the half-interval zones between the baffles.

4) The influence of the heat exchange intensification in the form of helical ribbing of the cylindrical baffle was studied using the computational flow dynamics inputs for the configuration 1 blade. It was possible to double the Nusselt number and the thermal transmittance values and to reduce the wall temperature by 54 °C in the most heat-loaded zone.

5) Using helical ribbing in the cylindrical baffle allowed to increase the thermal transmittance value by 33%, which may be used to reduce coolant consumption, which, in its turn, would result into greater cycle performance.

Acknowledgments

This study conducted by the Moscow Power Engineering Institute was financially supported by the Ministry of Science and Higher Education of the Russian Federation (project no. FSWF-2020-0020).

REFERENCES

1 Araujo G., Robalino-López A., Tapia N. Energy foresight: Exploration of CO_2 reduction policy scenario for Ecuador during 2016–2030. *Energetika.* 2019. Vol. 65, No 1, pp. 51 – 70.

2 Bariss U., Laicane I., Blumberga D. Analysis of factors influencing energy efficiency in a Smart Metering Pilot. *Energetika*. 2014. Vol. 60, No 2, pp. 125 – 135.

3 Energy I. World Energy Outlook 2014. International Energy Agency (IEA). OECD. Paris. IEA Publications, 2014. Available at: https://www.iea.org/reports/world-energy-outlook-2014

4 Kádár P. Pros and cons of the renewable energy application. *Acta Polytech. Hung*. 2014. Vol. 11, No 4, pp.211–224.

5 Phuangpornpitak N., Tia S. Opportunities and challenges of integrating renewable energy in smart grid system. *Energy Procedia*. 2013. Vol. 34, pp. 282 – 290.

6 Adar E. The State of the Art of Nuclear Energy: Pros and Cons. *EurAsia Waste Management Symposium*. Istanbul, 2020. pp. 26 – 28.

7 Boot-Handford M.E., et al. Carbon capture and storage update. *Energy Environ. Sci. Royal Society of Chemistry*. 2014. Vol. 7, No 1, pp. 130 – 189.

8 Rogalev A., et al. Research and Development of the Oxy-Fuel Combustion Power Cycles with CO2 Recirculation. *Energies.* 2021. Vol. 14, No 10, pp. 2927.

9 Scaccabarozzi R., Gatti M., Martelli E. Thermodynamic Optimization and Part-load Analysis of the NET Power Cycle. *Energy Procedia*. 2017. Vol. 114, pp. 551 – 560.

10 Rogalev A. et al. The flow path characteristics analysis for supercritical carbon dioxide gas turbines. *E3S Web of Conferences,* 2019. Vol. 124, pp. 01006.

11 Iwai Y. et al. Development Approach to the Combustor of Gas Turbine for Oxy-Fuel, Supercritical CO2 Cycle. *ASME Turbo Expo 2015*. Montreal, 2015. Vol. 9, pp. 1–7.

12 Allam R.J. et al. The Oxy-Fuel, Supercritical CO2 Allam Cycle: New Cycle Developments to Produce Even Lower-Cost Electricity From Fossil Fuels Without Atmospheric Emissions. *ASME Turbo EXPO 2014*. Düsseldorf, 2014. Vol 3B, pp. 1 – 9.

13 Allam R. et al. Demonstration of the Allam Cycle: An Update on the Development Status of a High Efficiency Supercritical Carbon Dioxide Power Process Employing Full Carbon Capture. *Energy Procedia*. 2017. Vol. 114, pp.5948–5966.

14 Sasaki T. et al. Development of Turbine and Combustor for a Semi-Closed Recuperated Brayton Cycle of Supercritical Carbon Dioxide. *ASME Turbo Expo 2017.* Charlotte, 2017. Vol. 1, 8 p.

15 Kindra V. et al. An experimental and numerical study of flow and heat transfer in cooling channels with pin fin-dimple and pin fin-groove arrays. *13 th European Conference on Turbomachinery Fluid dynamics & Thermodynamics*. Lausanne, 2018, pp. 1 – 10.

16 Ying Q. et al. Vortex Patterns Investigation and Enstrophy Analysis in a Small Scale S-CO2 Axial Turbine. *Energies*. 2021. Vol. 14, No 19, pp. 1 – 22.

17 Rahimi J., Poursaeidi E., Khavasi E. Stress analysis of a second stage gas turbine blade under asymmetric thermal gradient. *Mech. Ind. EDP Sciences.* 2019. Vol. 20, No 6, pp. 607.

18 Kim K.M. et al. Analysis of conjugated heat transfer, stress and failure in a gas turbine blade with circular cooling passages. *Eng. Fail. Anal*. 2011. Vol. 18, No 4, pp. 1212 – 1222.

19 Bohn D., Ren J., Kusterer K. Cooling Performance of the Steam-Cooled Vane in a Steam Turbine Cascade. *Turbo Expo 2005*. Reno, 2005. Vol 3, pp. 217 – 226.

20 Wróblewski W. Numerical evaluation of the blade cooling for the supercritical steam turbine. *Appl. Therm. Eng*. 2013. Vol. 51, No 1 – 2, pp. 953 – 962.

21 Kaewchoothong N. et al. Effect of inclined ribs on heat transfer coefficient in stationary square channel. *Theor. Appl. Mech. Lett*. 2017. Vol. 7, No 6, pp. 344–350.

22 Jin W. et al. Effect of shape and distribution of pin-fins on the flow and heat transfer characteristics in the rectangular cooling channel. *Int. J. Therm. Sci.* 2021. Vol. 161, 106758 p.

23 Gupta S., Chaube A., Verma P. Review on Heat Transfer Augmentation Techniques: Application in Gas Turbine Blade Internal Cooling. *J. Eng. Sci. Technol. Rev.* 2012. Vol. 5, No 1, pp. 57 – 62.

24 Aljibory M.W., Rashid F.L., Alais S.M.A. An Experimental and numerical investigation of heat transfer enhancement using annular ribs in a tube. *IOP Conference Series: Materials Science and Engineering*. 2018. Vol. 433, No 1, pp. 012057.

25 Yousefi A., Nejat A., Sabour M.H. Ribbed channel heat transfer enhancement of an internally cooled turbine vane using cooling conjugate heat transfer simulation. *Therm. Sci. Eng. Prog*. 2020. Vol. 19, pp. 100641.

26 Zheng N. et al. Effects of rib arrangements on the flow pattern and heat transfer in an internally ribbed heat exchanger tube. *Int. J. Therm. Sci. Elsevier*. 2016. Vol. 101, pp. 93–105.

Article accepted for publication 16.03.2022

.